PHYSICAL MECHANISMS DRIVING HARMFUL ALGAL BLOOMS ALONG THE TEXAS COAST

A Thesis

by

MARCUS TRISTAN OGLE

Submitted to the Office of Graduate Studies of
Texas A&M University
in partial fulfillment of the requirements for the degree of

MASTER OF SCIENCE

Approved by:

Chair of Committee,	Robert D. Hetland
Committee Members,	Lisa Campbell
	Matthew K. Howard
	Courtney Schumacher
Head of Department,	Piers Chapman

December 2012

Major Subject: Oceanography

ABSTRACT

Commonly referred to as “red tide”, harmful algal blooms (HABs) formed by *Karenia brevis* occur frequently in the Gulf of Mexico (GOM). A bloom is defined as cell abundances $>10^5$ cells L^{-1}. This thesis will focus primarily on *Karenia brevis*, formerly known as *Gymnodinium breve*, in the Gulf of Mexico. *K. brevis* is harmful because it produces brevetoxin, a ladder-frame polyether that acts as a potent neurotoxin in vertebrates. *K. brevis* commonly causes fish kills, respiratory irritation in humans, and Neurotoxic Shellfish Poisoning (NSP) if ingested. Blooms of *K. brevis* occur almost annually along the West Florida Shelf (WFS) in the late summer and early fall, when the coastal current is favorable for bloom initiation. Along the Texas-Louisiana shelf (TLS) however, blooms of *K. brevis* are infrequent and sporadic.

While much is known of the blooms along the WFS due to their frequent presence, little is known of the mechanisms driving the blooms along the TLS due to their inconsistent presence. To understand the stochastic nature of HABs along the TLS, historical data of bloom occurrences from 1996 to present were compared with NOAA station PTAT2 wind, sea-level pressure, air and water temperature data and NCEP NARR-A sea-level pressure data. The difference in the monthly-mean along-shore component of the wind was statistically significant between bloom and non-bloom years in September ($p<<0.001$) and April ($p=0.0015$), with bloom years having a strong downcoast current. Monthly mean water temperature values yielded similar results

between bloom and non-bloom years. Both March and September monthly-mean water temperature values were lower during non-bloom years with p-values of 0.01 and 0.048, respectively. These results suggest the possibly of forecasting for HABs along the TLS with currently measured, publicly available data.

DEDICATION

This thesis is dedicated to my parents, Eddy & Cynthia Ogle, who introduced me to the sea.

TABLE OF CONTENTS

LIST OF FIGURES

LIST OF TABLES

1. INTRODUCTION

1.1 General Circulation of the Gulf of Mexico

The subtidal annual and seasonal variability of the TLS circulation is predominantly forced by local surface momentum fluxes (wind stress) and buoyancy fluxes from rivers [Morey *et al.*, 2005; Nowlin *et al.*, 2005]. During the summer months (June, July and August), the climatologic wind pattern is from the south-east (Figure 1). These southerly winds result in an upcoast flow (land on the left in the Northern Hemisphere) in the direction opposite of the Kelvin wave due to Ekman transport. Figure 2 shows the mean 10m velocity stream functions for the TLS. In the summer months there is predominate upcoast flow across the entire shelf. In the non-summer months, the flow is downcoast near shore with weak upcoast flow at the shelf break (Figure 2) [Morey *et al.*, 2005; Nowlin *et al.*, 2005].

Along the eastern Gulf of Mexico, during the summer months, the flow is upcoast as a result of Ekman transport from the southerly winds. This southerly flow over the West Florida Shelf (WFS) brings nutrient rich waters from the Mississippi and Atchafalaya Rivers towards Florida and the Keys at depth of 20-50m [Stumpf *et al.*, 2008]. During the non-summer months, the flow is reversed and a downcoast flow is present.

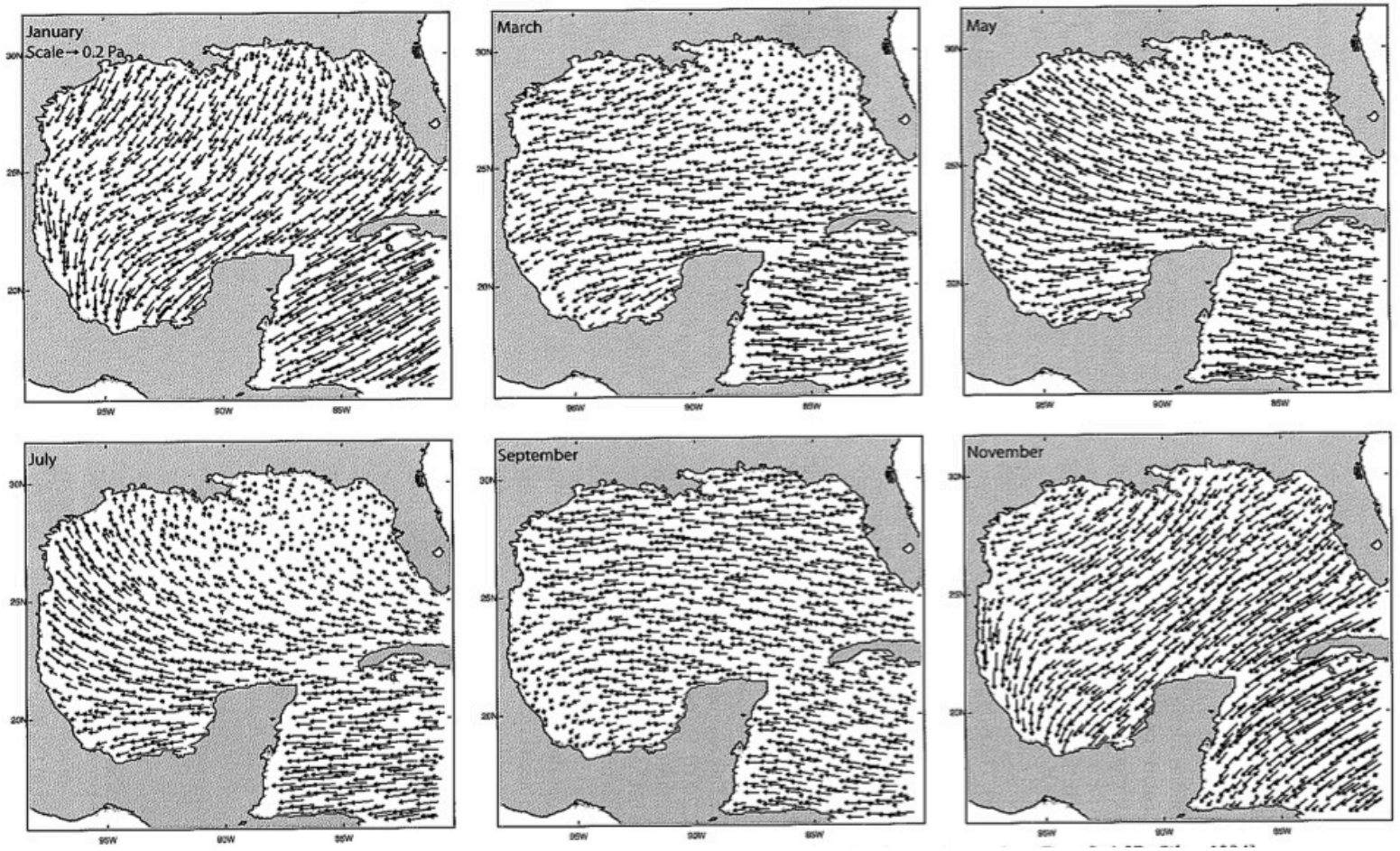

Figure 1: Monthly mean surface winds [Morey *et al.*, 2005]

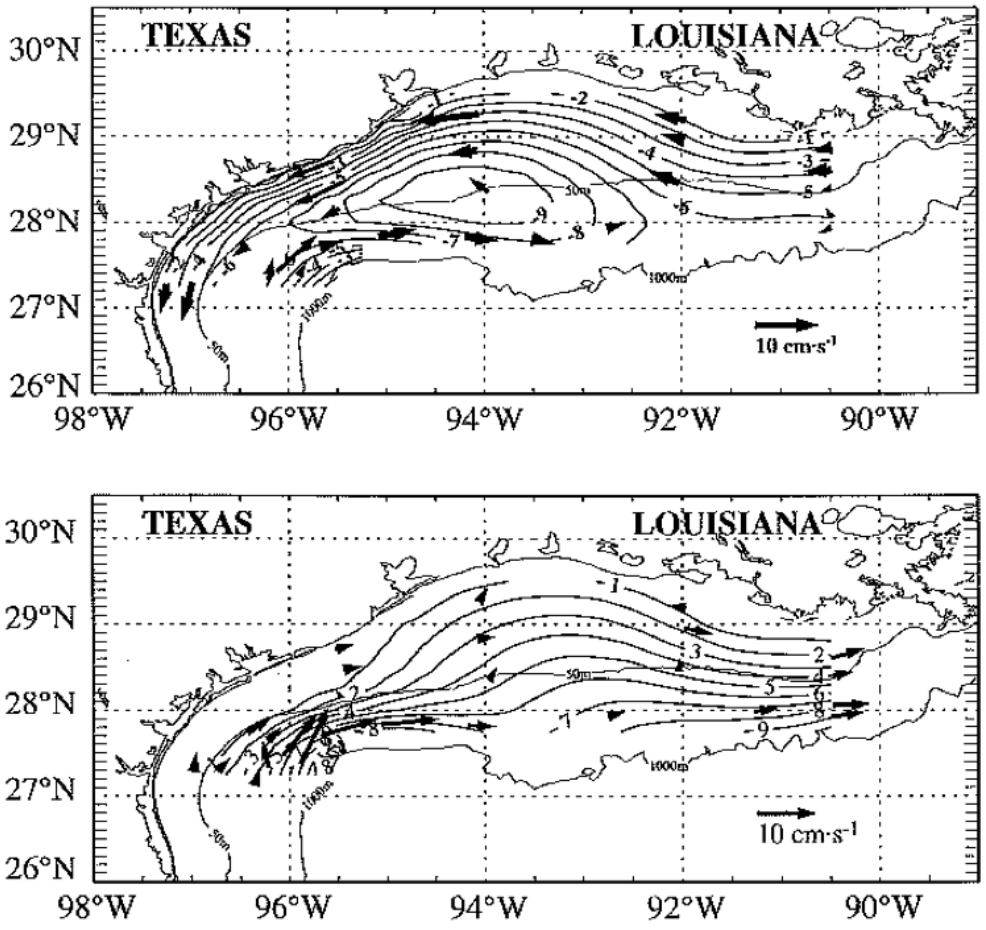

Figure 2: Mean 10m velocity stream field using LATEX observations. Non-summer months (top), summer months (bottom) [Cho, Ried and Nowlin, 1998]

The wind driven circulation across the TLS can be divided into three regions; near-shelf (region 1), far-shelf (region 2), and the open ocean (region 3) (Figure 3). Region 3 in this case is assumed to be infinite. As a northerly wind blows across the surface of the water, the net transport of the waters in Region 3 will be onshore due to Ekman drift. As Ekman drift persists, a barotropic raising of the sea-surface will occur in regions 1 and 2 due to the convergence associated with the onshore flow (Figure 3)

[Csanady, 1977]**.** At the bottom, an offshore flow becomes present to counteract the surface onshore flow caused by Ekman drift. The warm, light surface waters begin to downwell at the shore, thus lowering the thermocline. This lowering of the thermocline causes a further rise in the sea-surface height (SSH) as to maintain a constant pressure gradient. This baroclinic rising of the SSH is defined as Region 1. Region 2 typically extends to the shelf break. The raising of the sea-surface height across regions 1 and 2 induces an eastward pressure gradient, and as a result, a "costal jet" is formed with the strongest currents near-shore where baroclinic effects are present (Figure 3).

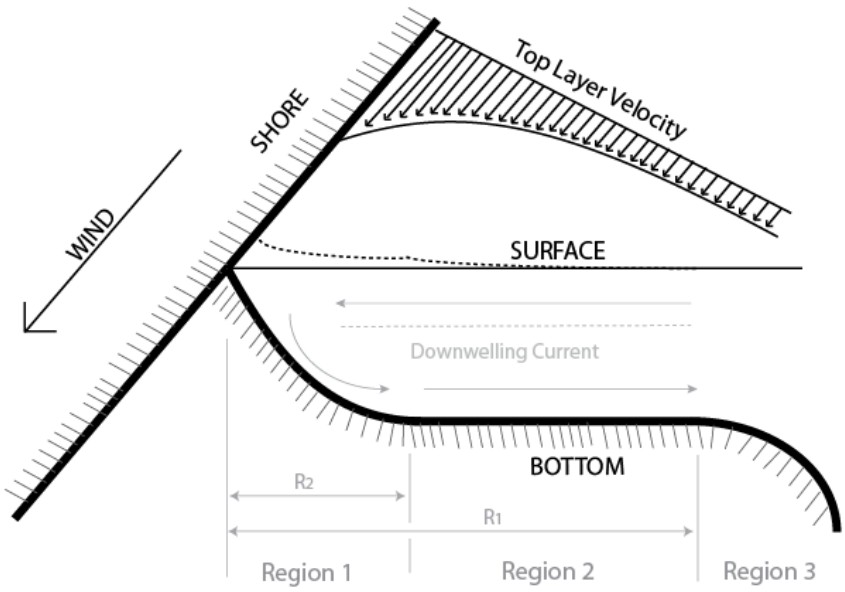

Figure 3: Wind driven circulation across a continental shelf, and the development of a coastal jet. [adapted from Csanady, 1977]

Wind stress is not the only factor in determining the flow along the shelf. Buoyancy fluxes from the atmosphere and rivers sets up pressure gradients, which result in currents. In the spring (March, April and May), the Mississippi and Atchafalaya Rivers are at their peak flow due to the draining of snow melt. The Mississippi and Atchafalaya Rivers contribute nearly two-thirds of the fresh water annually to the GOM [Dinnel and Wiseman, 1986; Etter *et al.*, 2004; Morey *et al.*, 2005]. This large flux of fresh water in the northern GOM in the spring, along with an increase in surface heating, sets up a large density gradient in the along shelf direction. This gradient would result in downcoast flow during the summer months, which, according to observations, is not the case. Nowlin *et al.* [2005] show that during the summer months, the upcoast flow is weaker when compared to the non-summer months, and this density gradient driving a downcoast flow could explain the weaker currents during the summer months (Figure 2).

The circulation patterns of the GOM have been heavily studied and well documented. The Loop Current (LC) aperiodically sheds anticyclonic mesoscale eddies within the GOM. The LC is part of the Gulf Stream; a western boundary current along the East Coast of the United States. These eddies have a vertical scale on the order of seven hundred meters, and due to potential vorticity conservation, are unable to make it onto the shelves and remain offshore [Morey *et al.*, 2005]. While eddies do not make it onto the shelves due to potential vorticity conservation, they do interact with shelf water at the shelf break by exchanging fluid between the outer shelf

and the deep ocean [Morey *et al.*, 2005; Nowlin *et al.*, 2005]. While there is no seasonal pattern on the chaotic nature of eddies, the exchange due to the presence of these eddies may be heavily influenced on the seasonal variability of shelf circulation and fluxes [Morey *et al.*, 2005].

1.2 West Florida Shelf

Blooms of *K. brevis* occur nearly annually along the WFS in the late summer and early fall [Stumpf *et al.*, 2008]. During the summer months, southerly winds result in eastward and southeastward flows, which brings nutrient rich river water from the Mississippi and Atchafalaya Rivers over the region (Figure 4; Stumpf *et al.*, 2008). Stumpf *et al.* [2008] believe the high inorganic and organic nitrogen concentrations in the river water promote the growth of *K. brevis* to pre-bloom concentrations in the sub-surface waters. The *in situ* growth of *Karenia* alone is not enough to develop a bloom where cell counts are $>10^5$ cells L^{-1} ; this suggests other factors, such as currents, aid in bloom initiation [Stumpf *et al.*, 2008].

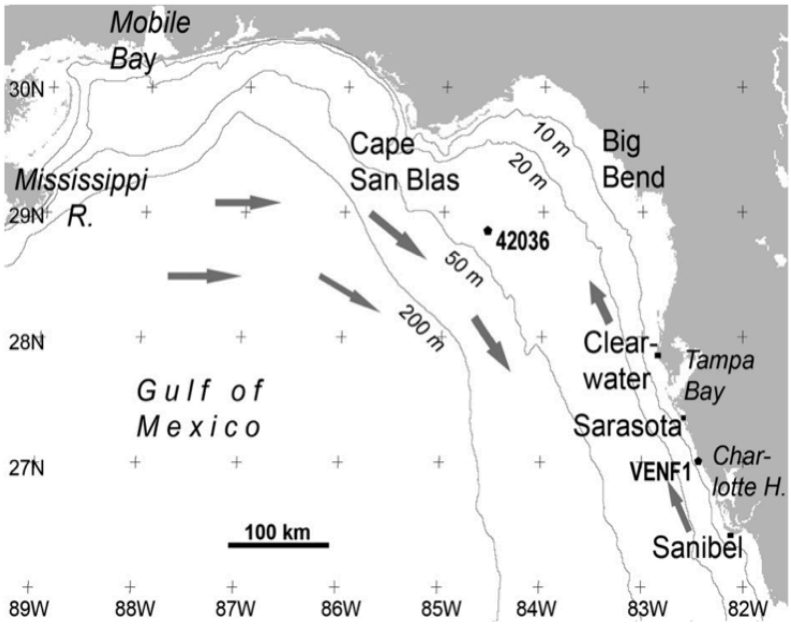

Figure 4: Summer circulation over the WFS [Stumpf et al., 2008]

In the late summer and fall, the winds begin to shift northerly, resulting in offshore flow over the WFS, yielding upwelling conditions. Under upwelling conditions, the subsurface *Karenia* are pushed onshore and begin to build in concentration. If the conditions last long enough, a bloom will form near-shore and at the surface, due to the upwelling event. These blooms can cover large spatial areas ranging from 10^2 km^2 to $>10^3$ km^2 and can last weeks to over a year in duration [Stumpf *et al.*, 2008]**.** *Karenia* has been shown to be phototactic when there is a surplus of nutrients, and chemotactic when they are nutrient limited [Heil, 1986; Liu *et al.,* 2001; McKay *et al.*, 2006]. During the day, *Karenia* tends to be phototactic because it is photosynthetic, and shows a net upward movement. At night, in the

absence of light, *Karenia* becomes chemotactic, and a net downward flux is seen. *Karenia* cells have the ability to swim down to a depth of 90m, where the waters are nutrient rich [Stumpf *et al.*, 2008]. Due to the upwelling conditions, the *Karenia* can remain near shore due to their vertical migration behaviors, and can explain why blooms can last for several days at a location.

Downwelling favorable winds can also yield surface blooms of *Karenia* if surface concentrations are already elevated. The onshore flow of the surface waters can pile up *Karenia*, and due to their phototactic behavior, can remain nearshore and near the surface, even during downwelling events. It has also been shown that downwelling currents near the bottom are significantly weaker than those during upwelling conditions, which would allow for those cells that came onshore during upwelling conditions to remain nearshore [Stumpf *et.al*, 2008; Hetland and Campbell, 2007].

Due to the near annual cycle of blooms along the WFS, a fairly accurate forecasting system has been developed using satellite observations from the Sea-Viewing Field-of-view Sensor (SeaWiFS), and heuristic and numerical models [Stumpf *et al.*, 2009]. The SeaWiFS aids in nowcasting of HABs through a heuristic model of cell counts and chlorophyll through ocean color imagery on a 1.1 km^2 pixel resolution at nadir (normal to the earth's surface) [Stumpf *et al.*, 2009; Stumpf *et al.* 2008]. Products such as total chlorophyll and chlorophyll anomaly allow for the ability to locate new blooms or to follow an existing bloom. Since chlorophyll anomaly is not species specific, several rules were set in place to determine the presence of *K. brevis*

[Stumpf *et al.*, 2009]. The SeaWiFs mission ended in December 2010, and has been replaced with MODIS, which is on-board both the Terra and Aqua spacecrafts[1]. MODIS covers a swath of 2,330 km by 10 km with a resolution of 1km for all ocean parameters[1].

While satellite imagery gives the widest field of view, there are several drawbacks; coarse resolution, not species specific, limited by cloud cover, and large uncertainties off nadir. Due to the resolution of sensors on SeaWiFS, it was only able to detect HABs when cell counts were >50,000 cells L^{-1} [Wynne *et al.*, 2005]. When the areas of interest were off nadir, chlorophyll concentrations could be overestimated by 1-3μgL^{-1} [Stumpf *et al.*, 2008]. In order to verify the presence of blooms, cell counts are required for validation of bloom species. Once a bloom was verified, the SeaWiFS was very accurate in allowing scientists to follow the bloom location.

In October 2004, a forecast model of intensification, transport, aerial extent and the impact of existing blooms on the coast was developed through the collaboration of NOAA and the state of Florida [Wynne *et al.*, 2008; Stumpf *et al.*, 2009]. While the model requires a bloom to be present, it has shown over 89% accuracy in its overall forecast ability, and 99% accuracy on coastal impact [Stumpf *et al.*, 2009].

[1] http://modis.gsfc.nasa.gov

1.3 Texas-Louisiana Shelf

While much research has been conducted along the WFS due to its annual cycle, very little has been done on HABs along the TLS. However, Magaña *et al.* [2003] collated data on historical blooms of *K. brevis* along the Texas and Mexican coasts. The first reports of "red water" are attributed to Alvar Nuñez Cabeza de Vaca, a chronicler aboard the Panfilo de Narvaez, which attempted to colonize the Gulf Coast in 1528. Table 1 shows a recent historical record gathered by Tester *et al.* [2004] of *K. brevis* events along the Texas and Mexican coasts. As one can see, HABs events have been present along the TLS and into Mexico, but are far more sporadic then those along the WFS.

While a system of routine sampling and monitoring is present along the WFS, no such system exists along the TLS. Samples on the state level are only taken in back bays and estuaries where the shellfishing industry is located, and only when reports of fish kills or other *K. brevis* symptoms appear [Wynne *et al.*, 2008]. The SeaWiFS algorithm used along the WFS proved to be inaccurate along the TLS due to the high concentration of organic materials in estuaries and frequent resuspension events offshore, which are interpreted as HABs. Wynne *et al.* [2005] reduced the number of false positives of offshore blooms by subtracting the reflectance from the red wavelength band from the chlorophyll anomaly detected by the SeaWiFS. This correction eliminated 43% of false positives for *K. brevis* from possible blooms from

1998 to 2002 [Wynne *et al.*, 2005]. However, just as the case with the WFS, blooms cannot be verified without samples being analyzed to confirm the presence of *Karenia*.

While no annual presences of *K. brevis* blooms have been reported along the TLS, it is possible that blooms offshore have been present. However, due to non-routine sampling of coastal waters, and the low resolution of satellite imagery, if these blooms were to be advected offshore, no signs of their presence would be noticed, and therefore would remain undocumented.

MEXICO	TEXAS
	1935 [a]
1946 [b]	1946–1947 [b]
1955 [c]	1955 [c]
1974 [d]	1974 [d]
	1986 [e]
1994–1995 [f,g]	
1996 [f,g]	1996 [h,i]
1997 [f,g]	1997 [h,j]
1999 [g]	1999 [i,j]
2000 [g,k]	2000 [j]
2001–2002 [k]	2001–2002 [k]

Sources of information: [a] Lund, 1936; [b]Gunter *et al.*, 1948; [c] Wilson and Ray, 1956; [d] Buskey 1996; [e]Trebatoski, 1988; [f] Sierra-Beltran *et al.*, 1998; [g] Marea Roja Foro Nacional, 2002; [h] Texas Dept. Health, 1997; [i] Texas Parks and Wildlife, 2000; [j] Texas Dept. Health, 2000; [k] Texas Dept. Health, 2001–2002.

Table 1: Historical record of *K. brevis* blooms along the Texas and Mexico gulf coasts [Tester *et al.*, 2004]

While blooms along both the WFS and TLS both occur in the late summer and early fall, their mechanisms for growth are very different. While it is well documented that blooms along the WFS initiate due to the high nutrient waters from the Mississippi and Atchafalaya Rivers being advected into the region due to Ekman transport, along the TLS, this is not the case. Villareal *et al.* [2001] suggested *K. brevis* initiation along

the Texas coast occurs >15km offshore and is surface advected nearshore. During the summer months, the southerly flow present over the GOM provides a sufficient mechanism for these surface populations to move nearshore and a bloom to occur. The high salinity bays and lagoons along the Texas coast also allow for these blooms of *Karenia* to make their way into these regions and allow for reoccurring and persistent blooms [Tester *et al.*, 2004].

1.4 Scientific Questions and Hypotheses

The WFS has been highly studied and a moderately accurate forecasting system has been in place since October 2004 [Wynne *et al.*, 2008]. This is not the case along the TLS, however. Prior studies show a definite need for a forecasting system along the TLS [Magaña *et al.,* 2003; Tester *et al.,* 2004; Wynne *et al.*, 2008; Stumpf *et al.*, 2009; Stumpf *et al.*, 2008]; however, the physical mechanisms driving the infrequent blooms over this region are not fully understood.

During the sixteen (16) year study period (1996-2011), eight (8) blooms were present and verified by the Texas Parks and Wildlife (TPWD) along the Texas coast in 1996, 1997, 1999, 2000, 2005, 2006, 2009, and 2011. The exact date of bloom initiation for all blooms is not known, but historically most blooms initiate sometime in late September to early/mid October. The following questions and hypotheses were assessed in this study:

1. What is the importance of temperature and salinity in bloom presence? Is there a difference in temperature and salinity between bloom and non-bloom years?

Hypothesis 1:

Sinclair *et al.* [2009], among others, and have shown *K. brevis* strive in warm, salty waters. From this knowledge, I draw my first null hypothesis: *there is no difference in water temperature nor salinity between bloom and non-bloom years.*

2. What is the role of wind on bloom presence? Is there a difference in the surface winds between bloom and non-bloom years?

Hypothesis 2:

The wind determines the strength of the prevailing current, along with its direction, through Ekman drift. Hetland and Campbell [2007] showed a mechanism for bloom initiation that is current driven. Using a numerical hydrodynamic model, Fei Chen [personal communication] showed similar results. Previous studies have shown that *K. brevis* growth rates alone are insufficient to create blooms of *K. brevis* along the Texas coast, suggesting dynamical factors are the primary cause for bloom initiation. *K. brevis* are assumed to remain near the surface, and are thus advected by surface currents. During downwelling conditions, *K. brevis* cells can become

aggregated near-shore, resulting in a bloom. With this knowledge, I draw my null second hypothesis: *There is no difference in the wind between bloom and non-bloom years*.

3. What is the role of sea-level pressure (SLP) in bloom dynamics? Is there a difference in SLP between bloom and non-bloom years?

Hypothesis 3:

During high SLP events, winds are typically suppressed and thus coastal currents are weaker. The opposite is true during low SLP events. Thus, high pressure and low-pressure center locations can play a major role on the strength and direction of the resulting winds. For instance, if a large high-pressure center were sitting over Florida, winds along the western GOM would be relatively strong and southerly, resulting in upwelling conditions. If this same high-pressure center were shifted westward, the resulting winds over the western GOM would still be southerly, but much weaker in strength. My third null hypothesis; T*here is no difference in SLP between bloom years and non-bloom years*.

2. DATA AND METHODS

2.1 Data

The major goal of this project was to determine a forecasting metric for blooms of *K. brevis* along the Texas coast. Values from March through September were used in the remainder of this study. This range was chosen because it was felt that any results found prior to March would be too big of an assumption for the corresponding fall, and the statistical power for forecasting would be too low.

2.1.1 Station PTAT2

Using the National Oceanic and Atmospheric Administration (NOAA) National Data Buoy Center (NDBC) website[2], data was collected for station PTAT2. Station PTAT2 is a C-MAN station with a MARES payload measuring: wind direction, wind speed, wind gust, air temperature, sea-level pressure, surface water temperature, wave height, wave period, wave spectra, relative humidity, dew point temperature, solar radiation, precipitation and visibility. For this study, I used: wind speed (WSPD), wind direction (WDIR), air temperature (ATMP), water temperature (WTMP) and sea-level pressure (SLP). Table 2 shows the range, frequency, averaging period, resolution and

[2] http://ndbc.noaa.gov

accuracy for each of the used parameters. I choose the most recent sixteen years (1996-2011) due to availability of data and the start date of WTMP measurements at this location.

Parameter	Range	Frequency (Hz)	Avg. Period	Resolution	Accuracy
Wind Direction	0 to 360	1.0	2 min	1 deg	+/- 10 dep
Wind Speed	0 to 62 m/s	1.0	2 min	0.1 m/s	+/- 1 m/s
Wind Gust	0 to 82 m/s	1.0	2 min	0.1 m/s	+/- 1 m/s
Air Temperature	-40 to 50 C	1.0	2 min	0.1 C	+/- 1 C
Pressure	800 to 1100 hPa	1.0	2 min	0.1 hPa	+/- 1 hPa
Sea Surface Temperature	-5 to 40 C	1.0	2 min	10.1 C	+/- 1 C
Wave Height	0 to 35m	1.71	20 min	0.1 m	+/- 0.2 m
Wave Period	0 to 30 sec	1.71	20 min	1 sec	+/- 1 sec
Wave Spectra	0 to 99 m*m/Hz	1.71	20 min	0.01 Hz	NA
Relative Humidity	0 to 100%	1.0	2 min	0.1%	+/- 6%
Dew Point Temperature	-35 to 30 C	1.0	2 min	0.1 C	+/- 1 C
Solar Radiation	0 to 2150 W/ m*m	1.0	2 min	0.5 W/m*m	+/- 5%
Precipitation	0 to 999 mm	continuous	6 hour	1 mm	5.0 mm
Visibility	0 to 8 mi	1.0	2 min	0.125 mi	+/- 10 %

Table 2: MARS Payload measurement statistics [http://www.ndbc.noaa.gov/rsa.shtml]

Station PTAT2 was chosen due to its location along the Texas coast (27.828 N, 97.050 W), and also because of its close proximity to Dr. Lisa Campbell's' Imaging Flow Cytobot (IFCB); an automated plankton classifier located on the University of Texas Marine Science Institute's pier in Port Aransas, Texas (Figure 5).

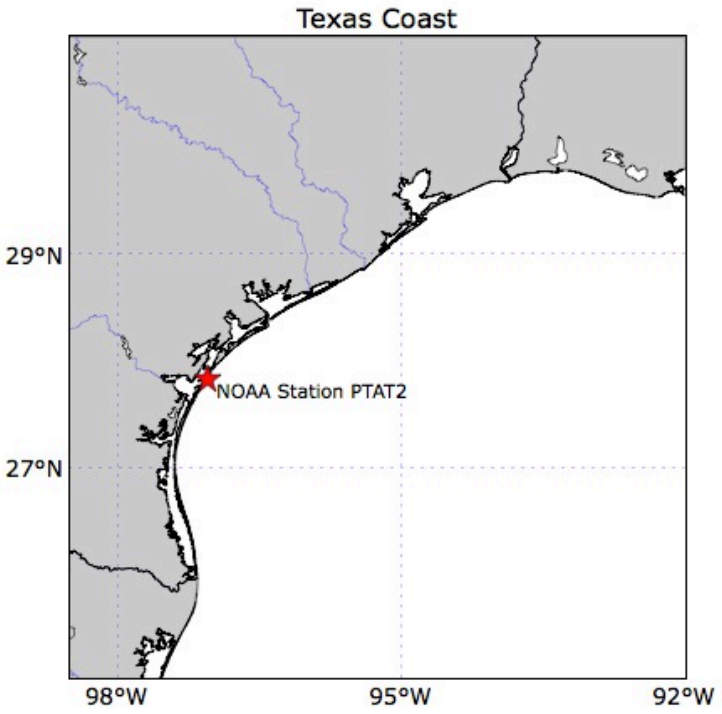

Figure 5: Location of NOAA Station PTAT2 along the Texas Coast (27.828 N, 97.050 W)

2.1.2 NCEP Reanalysis

Monthly-mean sea-level pressure data was obtained from Dr. Kenneth Bowman, Department of Atmospheric Science, Texas A&M University, who collected this data from the NOAA National Climatic Data Center (NCDC) website[3]. The grid spacing of this dataset is one-degree (1°) in both the 'x' and 'y' directions, covering the entire globe from 1948 to 2011.

[3] http://www.ncdc.noaa.gov

2.1.3 Drought Index

Because *K. brevis* has exhibited responses to varying temperature and salinity values, data from NOAA's Drought Information website[4] was gathered and analyzed in an attempt to find a correlation between Texas' drought condition and bloom presence along the Texas Coast. The Palmer Drought Severity Index uses temperature and rainfall information to determine dryness in a formula developed by Wayne Palmer in the 1960s. A value of zero reflects "normal" conditions, where a negative value represents drought condition, and a positive value represents excess rainfall.

2.2 Data Processing

Station data was gathered from the NDBC from January 1996 through December 2011. Yearly files were obtained and manually appended into one master file.

2.2.1 Winds

Using MatLab, WSPD and WDIR were loaded from the master data file. Over the sixteen-year period, there were three periods with major gaps. The first major gap is from 27 May 2001 through 6 June 2001. The second major gap is from 14 July 2006

[4] http://www.drought.noaa.gov

through 22 August 2006. The final gap is from 14 August 2007 through 19 September 2007.

One goal of this project was to determine whether or not the along-shore component of the wind has an affect on bloom presence. In order to calculate the along-shore component of the wind, several pre-processing steps were needed. As with all time series data, flagged values are present in the PTAT2 data. These values represent missing values and were '999' for both WSPD and WDIR. In order to not bias the data and average in values of '999', these flagged values were replaced with 'NaN'. Once all flagged values were replaced, the WDIR was be converted from the meteorological convention of zero-degrees (0°) being North and increasing clock-wise, to the mathematical convention of zero-degrees (0°) being East and increasing counter-clockwise. Equation 1 below was used for converting each value for WDIR into mathematical coordinates.

$$\Phi = (270 - WDIR) * (\pi/180) \quad (1)$$

Where Phi (Φ) is an array of the transformed wind direction values in radians.

The next step was to perform vector decomposition in order to separate the *u* and *v* components of the wind. Equations 2 and 3 were used to perform the decomposition,

$$u = \cos(\Phi) * WSPD \quad (2)$$

$$v = \sin(\Phi) * WSPD \quad (3)$$

where *u* represents the component of the wind in the East/West direction and *v* represents the component of the wind in the North/South direction. Since the along-shore component of the wind determines if the resulting currents are upwelling or downwelling favorable, it was necessary to rotate *u* and *v* to be oriented along the Texas coast at station PTAT2. Using Google Earth, an angle was calculated with station PTAT2 located in the center of a 100 mile line. The angle of the coast, theta (θ), was calculated to be roughly fifty-degrees (50°), or 0.87266 radians. *u* and *v* were then rotated using equations 4 and 5, respectively.

$$ur = u * \cos(\theta) - v * \sin(\theta) \quad (4)$$

$$vr = u * \sin(\theta) + v * \cos(\theta) \quad (5)$$

The values *ur* and *vr* are the rotated components of the wind with respect to the angle of the coast calculated above; theta (θ).

After the values had been rotated, monthly means were then computed. Sixteen dimensional arrays were created for each month (January through December), where each dimension was a different year. Because we were only interested in the along-shore component, only *ur* values were used. Each individual monthly array of *ur* was then placed into a master array for further analysis.

2.2.2 Temperature

Water and air temperature values were similarly arranged as the wind data in section 2.2.1. The gaps in data, as discussed in the previous section, were also in both the water and air temperature time series. However, from 1 January 1996 to 1 May 1996 no water temperature measurements were made.

Unlike the wind data, neither the air nor water temperature values needed to be rotated. The replacement of flagged values with 'NaN' was necessary as not to compute values of '999' into the monthly averages.

2.2.3 Sea-Level Pressure

Sea-level pressure data from station PTAT2 was arranged just as the temperature and wind data as before. Monthly means were calculated after replacing flagged values with 'NaN'.

Sea-level pressure data from the monthly-mean NCEP Reanalysis dataset was straightforward. Data was from 1980 to 2011 was loaded into Python and various statistical techniques were performed. Between 1980 and 2011, there were eleven reported HAB events along the Texas coast in 1986, 1990, 1996, 1997, 1999, 2000, 2001, 2005, 2006, 2009 and 2011.

2.2.4 Salinity

When searching for a correlation between bloom presence and salinity, I first looked at rainfall data. Sinclair *et al.* [2009], among others, showed a dependence between salinity and growth rates of *K. brevis*, where higher salinities yield a higher growth rate. Seven major river systems flow into the Gulf of Mexico. The salinity of coastal and bay waters along the Texas coast show a positive correlation between freshwater input from these river systems and the resulting salinities of the waters. Data were collected from NOAA's Drought Information website; specifically the Palmer Drought Severity Index (PDSI).

Data from January 1955 through December 2010 was collected for the state of Texas. The file contains monthly averages of rainfall and temperature, and the resulting PDSI, along with others. This data was then loaded into a Python script of analysis.

Because blooms of *K. brevis* typically occur in the early fall months, summer values were assessed for this study. June, July, August and September PDSI values were averaged and arranged in numerical order. An array of years was also created and ordered in rank according to the PDSI.

3. RESULTS

One-way ANOVA (Analysis of Variance) calculations were performed for each of the four parameters below.

3.1 Winds

Figure 6 is a time series plot of the monthly average of *ur* ($\overline{ur}$) and shows a general trend of positive values (upcoast) during the summer months and negative values (downcoast) during the remainder of the year. This result is in agreement with Morey *et al.* [2005] and Nowlin *et al.* [2005]. To determine if there is a difference between bloom and non-bloom years, averages and standard deviations were then computed for each month for bloom and non-bloom years (Figure 7). The dashed black line represents years where no bloom was detected along the Texas coast, and the solid red line are years where a bloom was detected. It is evident that there is a difference in the along-shore component of the wind between bloom and non-bloom years in September, August and April, but are these differences significant? To answer this question, one-way ANOVA were performed.

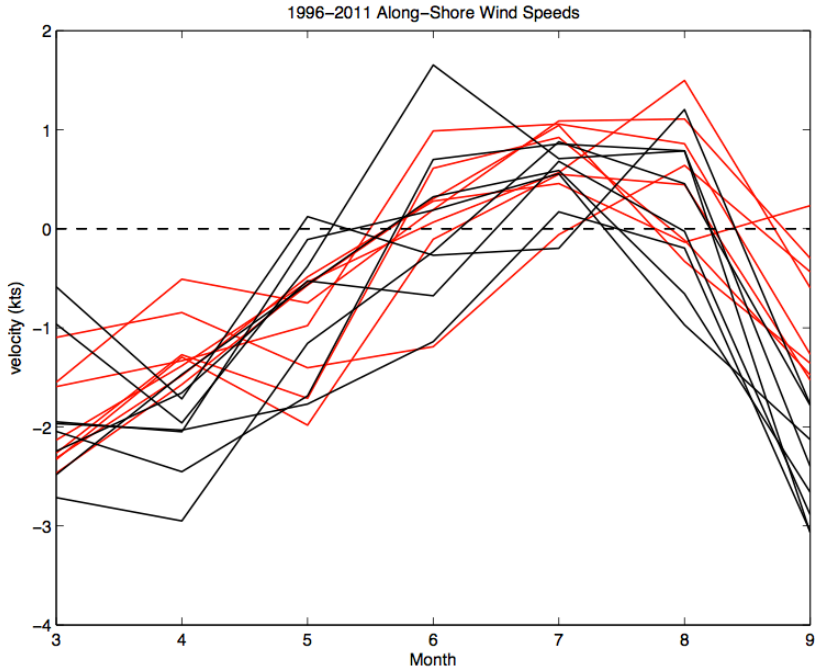

Figure 6: Along-shore wind speeds for all years (1996-2011). HAB (red) and non-HAB (black) years

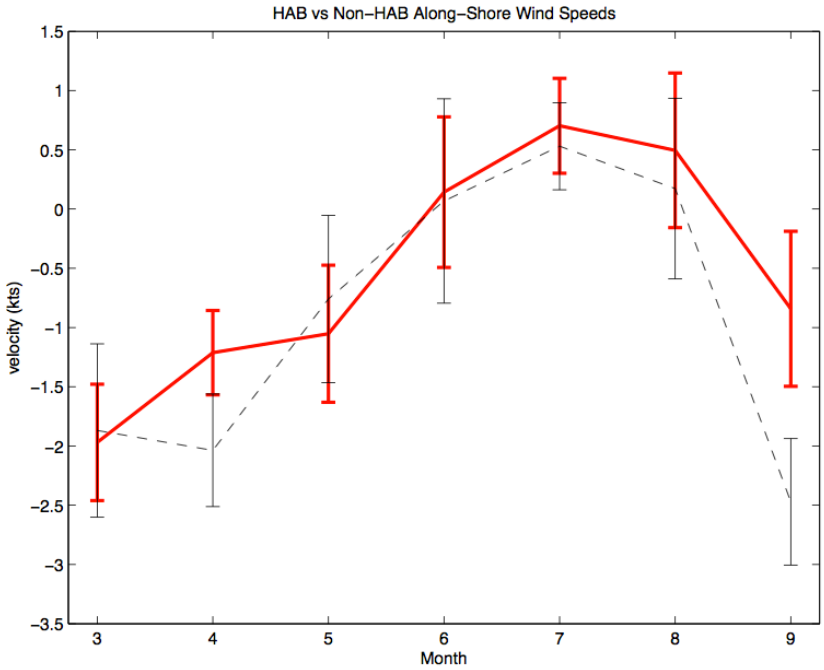

Figure 7: Monthly mean along-shore wind speeds with standard deviations. HAB (solid red) and non-HAB (dashed black) years

Before performing the ANOVA on the September $\overline{ur}$ values, the September values were plotted for each year and color-coded for visual inspection. Figure 8 is the September along-shore wind speeds for each of the years in the analysis period. The red asterisks represent years in which a HAB event occurred, and the black crosses represent years in which no HAB event was recorded. From this figure, there appears to be a clear distinction of the along-shore wind speed between bloom and non-bloom years. During years where there was strong downwelling, no HAB events were recorded along the Texas coast, and in years where there were weakly downwelling currents, HAB events were reported during the analysis period.

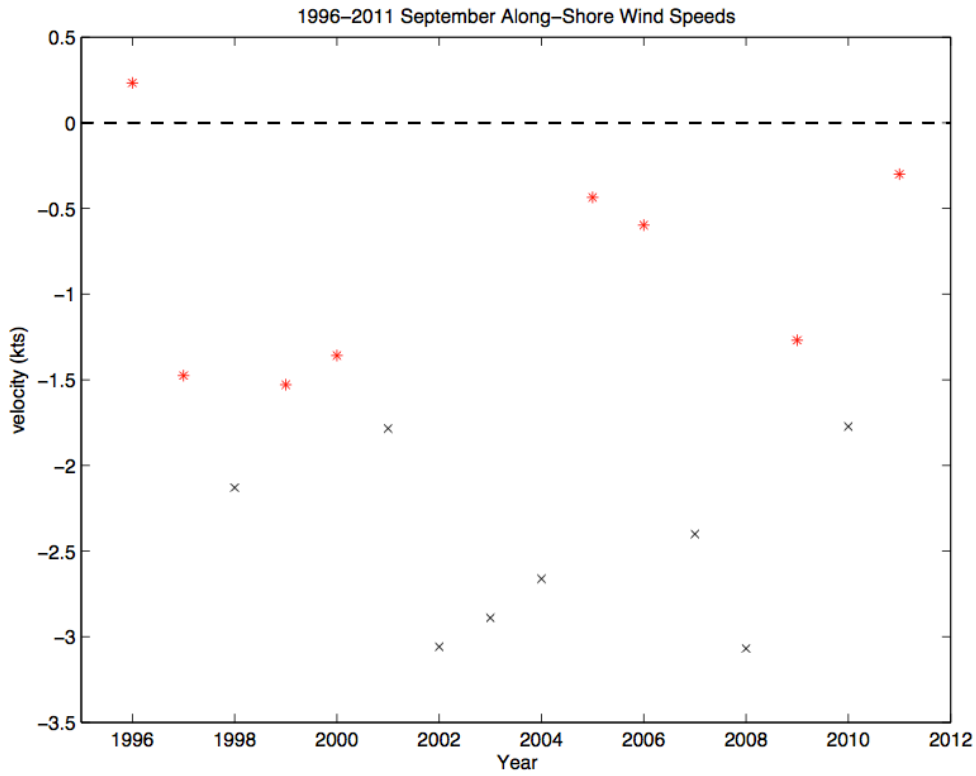

Figure 8: September mean along-shore wind speed. HAB (red asterisk) and non-HAB (black crosses) years

The one-way ANOVA for the September $\overline{ur}$ values yields greater than 99% confidence that the two periods' means (bloom vs. non-bloom years) are significantly different with p<<0.001 (Figure 9).

The same ANOVA technique was applied to the other months in the data set (March thorough August). Figure 7 shows a difference between bloom and non-bloom years for April, and the one-way ANOVA yielded a p-value of 0.0015 (Figure 10) [5]. The small difference noticeable for August in Figure 7, yielded no significance in the difference between bloom and non-bloom years.

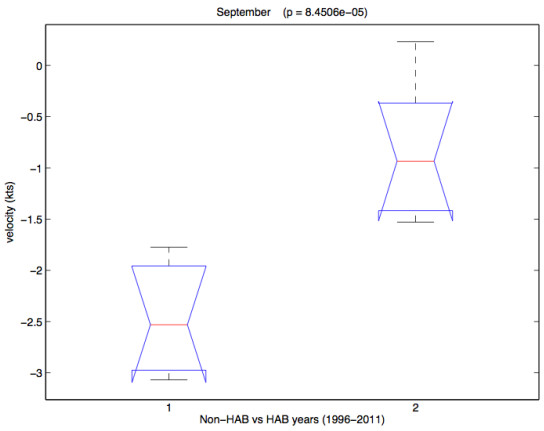

Figure 9: September along-shore wind speed ANOVA output. Non-HAB years (1) and HAB years (2)

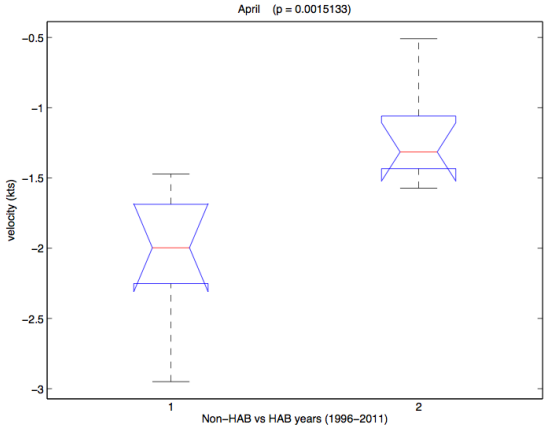

Figure 10: April along-shore wind speed ANOVA output. Non-HAB years (1) and HAB years (2)

[5] Interpreting the ANOVA box plot: The red line represents the median of the data. The notch represents the 95% confidence interval. The whiskers represent the range of values in the data set that are not considered outliers. The horizontal blue lines represent the 25% and 75% quartiles.

3.2 Temperature

When working with water temperature data from PATA2, there was enough evidence to reject the null hypothesis on a 95% confidence level for both the September (p=0.048) and March (p=0.011) monthly mean water temperature values. Figures 11 and 12 are the March and September one-way ANOVA output, respectively.

When these methods were applied to the monthly mean air temperature readings, there was no statistical difference between bloom and non-bloom years.

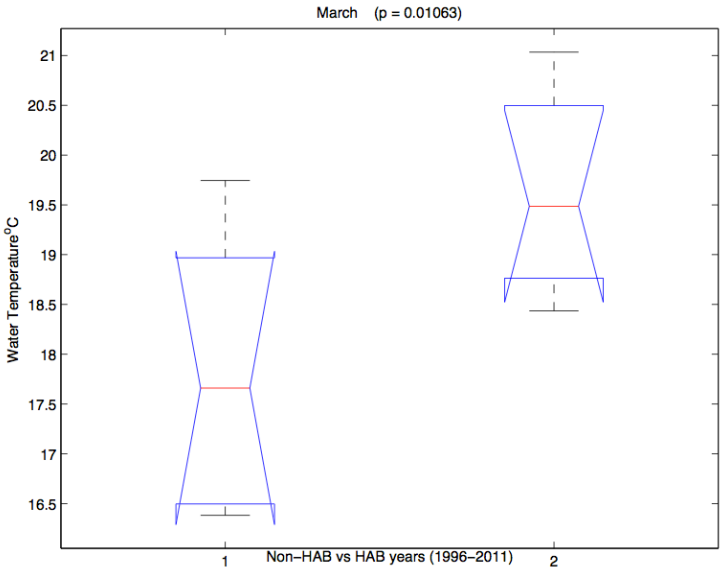

Figure 11: March water temperature ANOVA output. Non-HAB years (1) and HAB years (2)

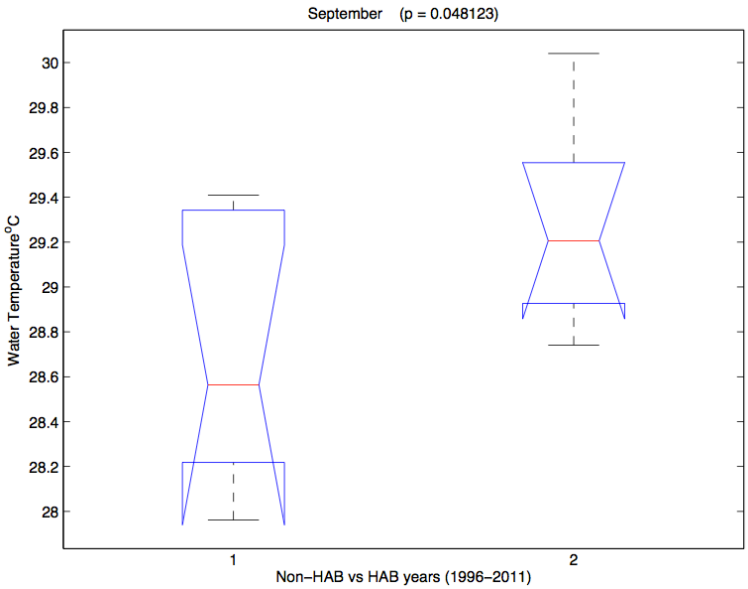

Figure 12: September water temperature ANOVA output. non-HAB years (1) and HAB years (2)

3.3 Salinity

In an attempt to use the readily available Palmer Drought Severity Index (PDSI) as an indicator for bloom forecasting along the Texas Coast, the summer mean PDSI was ranked numerically with the corresponding year being flagged as a bloom or non-bloom year. Figure 13 is the time series plot of the summer mean PDSI with HAB years indicated with a larger red marker.

Negative PDSI values indicate times of drought while positive values indicate times of excess rainfall. There appears to be no clear correlation between Texas drought conditions and bloom presence along the Texas coast, so using the PDSI as an indicator for bloom forecasting does not seem feasible.

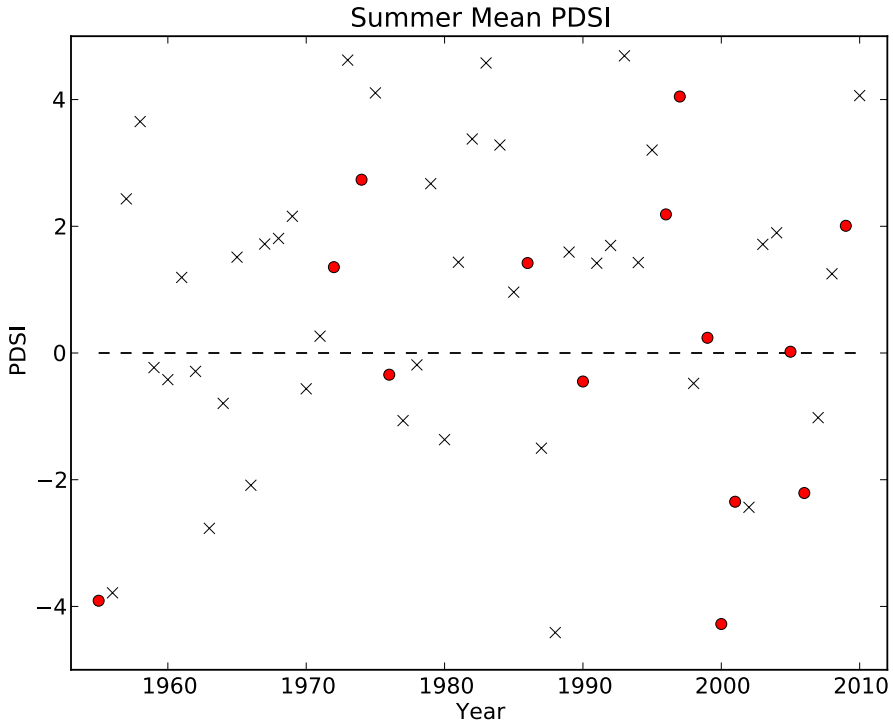

Figure 13: Summer PDSI time series. HAB (red dots) and non-HAB (black crosses) years

3.4 Sea-level Pressure

3.4.1 Station PTAT2

Sea-level pressure data from NOAA station PTAT2 was also testing using the one-way ANOVA technique just as the wind and temperature data as above. A time series plot of the monthly mean SLP for each year shows a general trend of higher pressure in the winter (December, January and February) and summer (June, July and August) months with lower pressures the remainder of the year (Figure 14).

When looking at the monthly means for bloom and non-bloom years (Figure 15), there does appear to be a difference in SLP in March, April and September. The one-way ANOVA output for March yielded a significant difference between bloom and non-bloom years on the 90% confidence level, with higher pressures during HAB years (Figure 16). There was no difference between bloom and non-bloom years for April nor September.

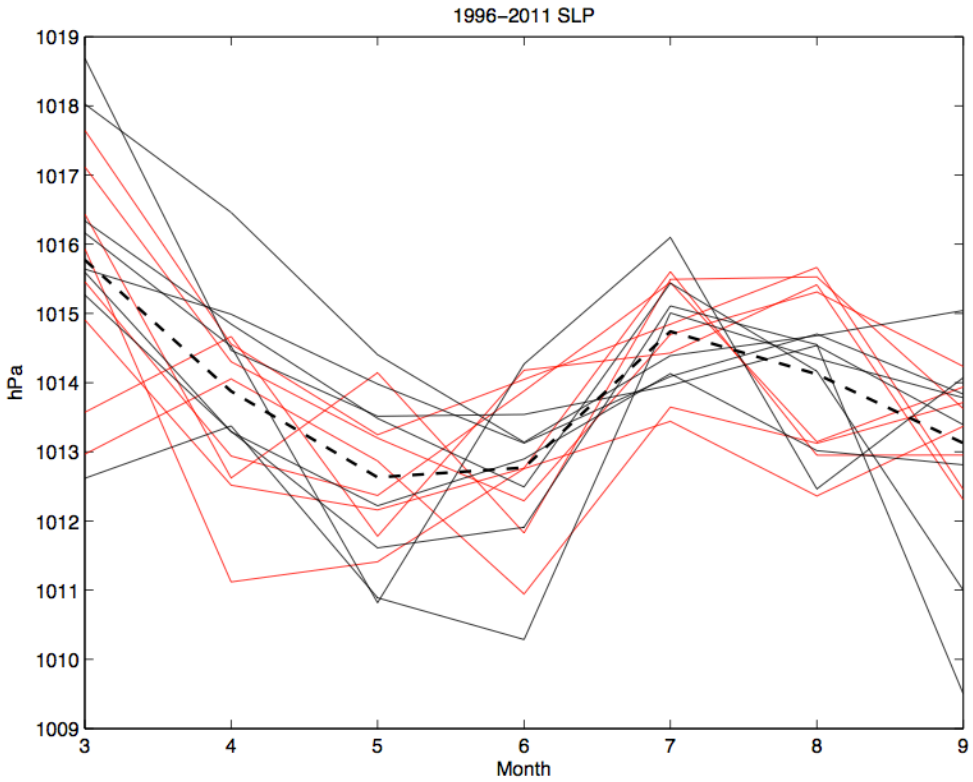

Figure 14: Monthly mean SLP time series (1996-2011). The monthly average across all years is indicated by the black dashed line; HAB (red) and non-HAB (black) years

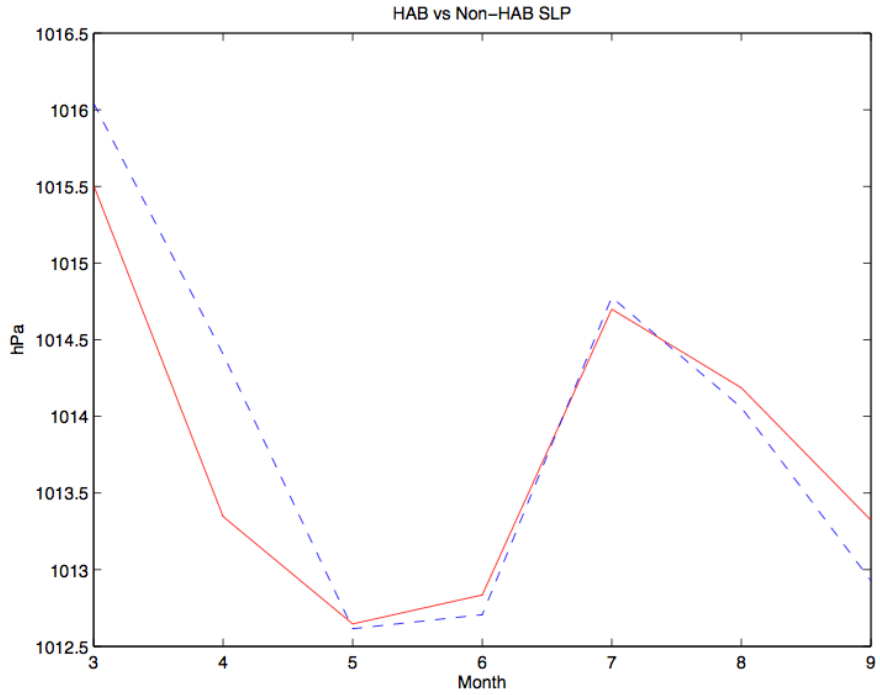

Figure 15: Monthly mean SLP time series. HAB (dashed blue line) and non-HAB years (solid red line).

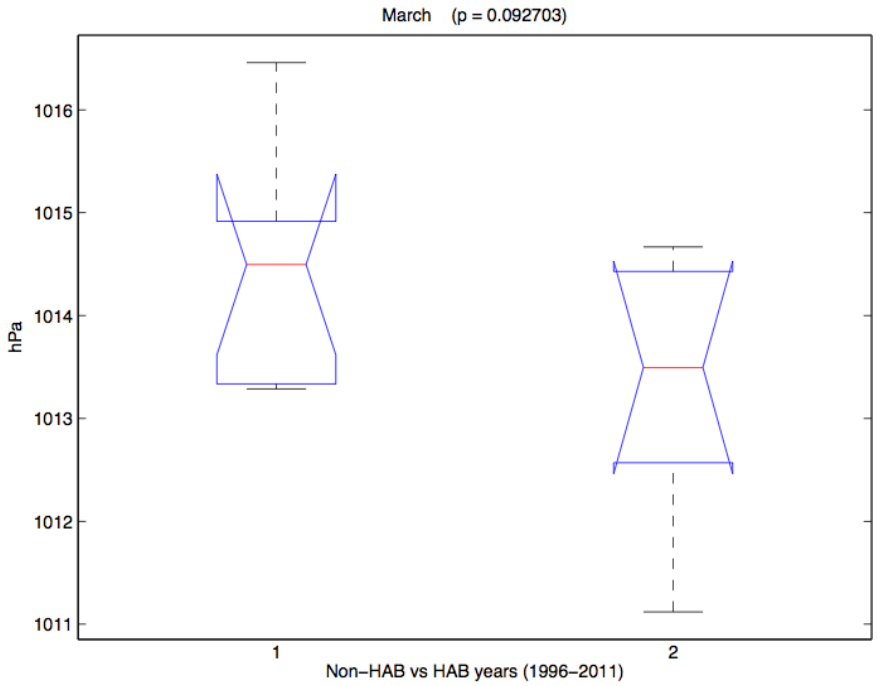

Figure 16: March SLP ANOVA output. non-HAB (1) and HAB years (2)

3.4.2 NCEP Reanalysis

The gridded monthly NCEP Reanalysis SLP data for North America was plotted for March; the month found in section 3.4.1 to have significantly different means between bloom and non-bloom years. Figure 17 is the March SLP pressure map covering North America, comparing HAB and non-HAB years from 1980 to 2011. I expected an obvious difference in High and Low pressure centers and strength would be present in the plots of SLP however, there appeared to be no major difference in the location and strength of the local high and low pressure centers over North America for March.

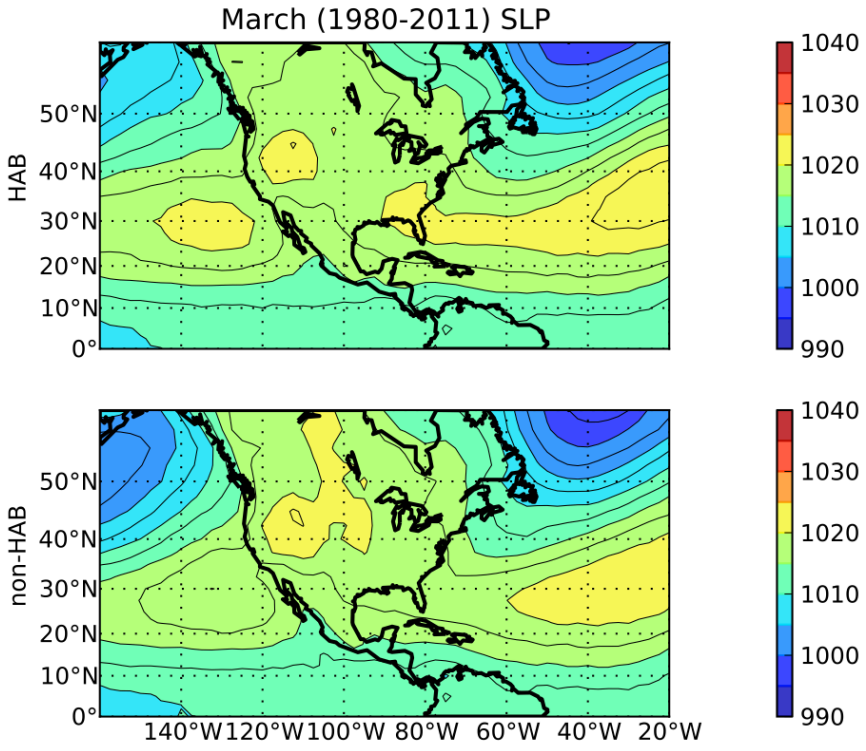

Figure 17: Average March SLP from 1980 to 2011 (HAB and non-HAB years

Further analysis of this dataset was done, but for the entire northern hemisphere; again from 1980 through 2011. In order to provide statistical power to the results, p-values were calculated between bloom and non-bloom years for each grid point, then plotted. Figure 18 is the March SLP p-values between HAB and non-HAB years. There are four regions where the results were significant ($p<0.02$): over central Africa, in the mid-Atlantic off the horn of Africa, the Caribbean Sea, and over the Beaufort Sea. Another area of possible interest was in the North Pacific Ocean, just off the Aleutian Islands. Other months yielded areas where the difference in SLP between bloom and non-bloom years was significant, but none were as dramatic as the results for March.

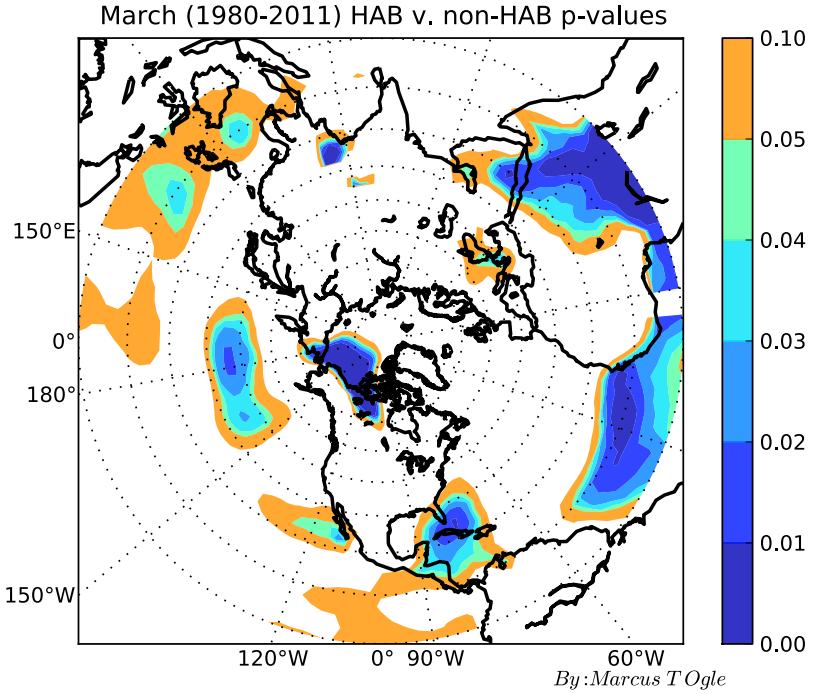

Figure 18: March SLP p-values for HAB and non-HAB years

4. DISCUSSION

Much research has been done on the topic of *Karenia spp.* over the last 50 years, but little has been about bloom dynamics , i.e., how blooms form. Several have speculated, and even tried to model, growth rates as factors of temperature, light, salinity and nutrients, but none have produced results consistent with blooms found in nature. Salinity, temperature, light nor nutrients can explain the 100 fold, or greater, in cell concentration found during bloom events that can occur in just a few hours time [Aldrich and Wilson, 1960; Shanley, 1985; Shanley and Vargo, 1993; Eng-Wilmont *et al.,* 1977; Sinclair *et al.,* 2009].

Aldrich and Wilson [1960] and Wilson [1966] showed that in laboratory experiments, *G. breve* (now known as *Karenia brevis*) had optimal growth between salinity values of 27 to 37 ppt, with a reduction in growth below 24 ppt. Steidinger [1998] later found the optimal growth of *K. brevis* to occur around 35 ppt, salinity.

Errera and Campbell [2011] looked more into the salinity issue by measuring the responses of *K. brevis* in environments of changing salinities. They showed that hypoosmotic stress (oceanic→coastal conditions; 35→27 ppt), brevetoxin concentration within the cell increased up to 53%, while there was no change in growth rate. Under hyperosmotic stress (coastal→oceanic conditions; 25→35 ppt), a similar increase in brevetoxin content decreased significantly. Errera and Campbell [2011] also observed an increase in cross-sectional area (CSA) under hypoosmotic stress, and

observed a 5% increase in CSA after 3h; by 24h the cells had returned to equal the size of the control group. One interesting thing they found was the continued increase in brevetoxin levels 6 days after hypoosmotic stress. These findings, along with those found by Aldrich and Wilson [1960], Wilson [1966] and Steidinger [1972], and the absence of reliable and continuous salinity measurements, led me to not purse a connection between salinity and HAB events along the Texas coast.

I chose to use monthly mean values of wind instead of higher frequency values, because the weather band scale is not long enough to greatly impact the large scale circulation along the Texas coast. Zhang *et al.* [2012] and Weaver and Nigam [2007] conclude that weather band processes (ie. frontal passages, hurricanes, etc.) alter coastal currents, but only on short time scales (hours to days). The larger, monthly-mean timescale dominates the circulation pattern over the region. They also point out that weather band processes have less effect on the coastal current during the summer months due to the weak strength of those processes during the summer months. Zhang *et al.* [2012] conclude that no temporal patterns can be concluded from weather band wind data, while a clear seasonal pattern is present using the monthly-mean wind data. While weather band process can affect the exact timing of a bloom, it would not be helpful as a predictor several months out, since there is no obvious pattern to weather band processes and they are too short temporally.

While I have discounted salinity and weather band processes for this study, I do feel more research needs to be done before these factors can be completely ignored for

future HAB monitoring. Due to the lack of a salinity time series along the Texas coast, it would be hard to completely dismiss salinity as a predictor for HAB events, especially since *K. brevis* is a tropical marine algae. While I do not feel weather band processes are useful in creating long term forecasts for HAB events, I do feel they would be useful in short term forecasts once a bloom has been verified offshore.

5. CONCLUSIONS

Over the sixteen-year period analyzed from the PTAT2 data, eight (8) years contained blooms of *K. brevis*: 1996, 1997, 1999, 2000, 2005, 2006, 2009, and 2011.

It was shown that the along-shore component of the wind drives coastal circulation over the western GOM and thus this metric was tested. Significance was found for both April and September winds between bloom and non-bloom years. In years with blooms, weaker downwelling conditions in both April and September were found. The weaker downwelling conditions in September are more favorable for bloom initiation due to the phototaxic nature of *K. brevis* and their ability to swim against the downwelling coastal current. The stronger downwelling conditions present in years without a bloom produce a strong coastal current, which, I believe, act to flush out the *K. brevis* bloom that could be present otherwise.

It was also shown that the September presence of *K. brevis* blooms are significantly correlated with warmer water temperatures in both September and during the previous March. The warmer water temperatures allow for *K. brevis* to grow at a near optimal rate. When looking at air temperature, no strong conclusions could be drawn between bloom years and non-bloom years, suggesting ocean processes are the cause for bloom events along the Texas coast.

The Palmer Drought Severity Index was analyzed as a forecasting metric for bloom presence along the Texas coast, but no conclusive evidence could be found. Blooms were present in all drought conditions, so this analysis was abandoned.

The final hypothesis that there is no difference in SLP between bloom and non-bloom years, was tested. Just as with air temperature, this hypothesis was not rejected on the 95% confidence level, however a p-value of 0.0927 was achieved for March. While there is a significant difference with 90% confidence in SLP between bloom and non-bloom years, the difference in means is roughly 2 hPa in March and 0.8 hPa in September. Due to the small range, I feel the power of this test not enough to provide a confidence forecast for HABs.

As previously stated, I do believe SLP plays a large role in bloom presence, but the PTAT2 data only includes SLP strength and not the location of the large pressure systems driving the SLP in Port Aransas, Texas. PTAT2 data only contains SLP in Port Aransas, so NCEP Reanalysis data from 1980 through 2011 was analyzed to allow for a global view of SLP.

P-values were calculated from the NCEP Reanalysis monthly mean SLP data, and plotted for the northern hemisphere. Four areas stood out as having large areas of high significance ($p<0.05$) in March; central Africa, the mid-Atlantic off the horn of Africa, the Caribbean Sea, and over the Beaufort Sea. Of the four (4) areas, the area over the Caribbean Sea is the most likely to have the largest affect on blooms of *K. brevis* along the Texas coast. The strength of the SLP over the Caribbean Sea can alter the flow of

the resulting winds. In years where no bloom was detected, the March mean SLP is lower than in years when a bloom was detected (section 3.4.1). If the SLP over the Caribbean is higher than in other years, southerly winds will be stronger along the Texas coast and oppose the climatologic easterly winds over the region. A weaker downwelling current will then be present along the Texas coast. A weaker SLP over the Caribbean would not oppose the climatologic easterly winds, thus not inhibit the downwelling current historically present.

The one main goal of this project was to determine a metric to aid in forecasting for blooms of *K. brevis* along the Texas coast. With a p-value of 0.0015, I feel confident in using the April mean along-shore winds as a predictor for future bloom presence for that year. I also feel confident in using the mean water temperature value for March as a predictor (p=0.011). One convenient conclusion is that April follows March, so if the conditions are favorable in March and again in April, I would feel very confident in the likelihood of a HAB event later that year.

REFERENCES

Aldrich, D.V. and W.B. Wilson (1960), The effects of salinity on growth of *Gymnodinium breve* Davis, Biol. Bull 119, pp. 57-64.

Baden, D. (1989), Brevetoxins: unique polyether dinoflagellate toxins, FASEB, Vol. 3, pp. 1807-1817, doi:0892-663818910003-18071$01.50.

Cho, K., R.O.R.Y. Thompson, and W. D. Nowlin (1998), Objectively mapped stream function fields on the Texas-Louisiana shelf based on 32 months of moored current meter data, J. Geophys. Res., 103(C5), pp. 10377-10390.

Csanady, G. T. (1977), The Coastal Jet Conceptual Model in the Dynamics of Shallow Seas, in The Sea, Volume 6: Marine Modeling, edited by E. Goldberg, I. McCave, J. O'Brien, and J. Steele, pp. 117-129, Harvard University Press, Cambridge, Mass.

Dinnel, S. P. and W. J. Wiseman, Jr. (1986), Freshwater on the Louisiana and Texas shelf, Cont. Shelf Research, Vol. 6, pp. 765-784.

Eng-Wilmont, D.L., W.S. Hitchcock, and D.F. Martin (1977), Effects of temperature on the proliferation of *Gymnodinium breve* and *Gomphosphaeria aponina*, Mar. Biol. 41, pp. 71-77.

Errera, R. and L. Campbell (2011) Osmotic stress triger toxin production by the dinoflagellate *Karenia brevis*, PNAS, 108, pp. 10597-10601.

Etter, P. C., M. K. Howard, and J. D. Cochrane (2004), Heat and freshwater budgets of the Texas-Louisiana shelf, J. Geophys. Res., Vol. 109, C02024, 24 pp., doi: 10.1029/2003JC001820.

Heil, C. A. (1986), Vertical Migration of *Ptycodiscus brevis* (Davis) Steidinger, University of South Florida, Tampa, Florida, Unpublished.

Hetland, R. and L. Campbell (2007), Convergent blooms of Karenia brevis along the Texas coast, Geophysical Research Letters, Vol. 43, L19604, doi: 10.1029/2007GL030474.

Liu, G., G. S. Janowitz, and D. Kamykowski (2001) The influence of environmental nutrient condition on *Gymnodinium breve* (Dinophyceae) population dynamics: a numerical study, Marine Ecology Progress Series 213, pp. 13-37.

Magaña, H. A., C. Contreras, and T. A. Villareal (2003), A historical assessment of Karenia brevis in the western Gulf of Mexico, Harmful Algae 2, pp. 163-171, doi: 10.1016/S1568-9883(03)00026-X.

McKay, L., D. Kamykowski, E. Milligan, B. Schaffer, and G. Sinclair (2006), Comparison of swimming speed and photophysiological responses to different external conditions among three Karenia brevis strands, Harmful Algae 5, pp. 623-636, doi:10.1016/j.hal.2005.12.001.

Morey, S. L., J. Zavala-Hidalgo, and J. J. O'Brien (2005), The Seasonal Variability of Continental Shelf Circulation in the Northern and Western Gulf of Mexico From a High-Resolution Numerical Model, in Circulation in the Gulf of Mexico: Observations and Models, edited by W. Sturges and A. Lugo-Fernandez, pp. 203-218, AGU, Washington, D.C.

Nowlin, W. D., A. E. Jochens, S. F. DiMarco, R. O. Reid and M. K. Howard (2005), Low-Frequency Circulation Over the Texas-Louisiana Continental Shelf, in Circulation in the Gulf of Mexico: Observations and Models, edited by W. Sturges and A. Lugo-Fernandez, pp. 219-240, AGU, Washington, D.C.

Shanley, E. (1985), Photoadaptation in the red-tide dinoflagellate *Ptychodiscus brevis*, M.S Thesis, 122 p., Univ. South Florida.

Shanley, E. and G.A. Vargo (1993), Cellular composition, growth, photosynthesis, and respiration rates of *Gymnodinium breve* under varying light levels, in Toxic Phytoplankton Blooms in the Sea, edited by T.J. Smayda and Y. Shimizu, pp. 831-836, Elsevier, NY.

Sinclair, G., D. Kamykowski, and P. M. Gilbert (2009), Growth, uptake, and assimilation of ammonium nitrate, and urea, by three strands of Karenia brevis grown under low light, Harmful Algae 8, pp. 770-780, doi:10.1016/j.hal. 2009.02.006.

Steidinger, K. A. and R.M. Ingle (1972), Observations on the 1971 red tide in Tampa Bay, Florida, Environ. Letters 3, pp. 271-278.

Steidinger, K. A., G. A. Vargo, P. A. Tester, and C. R. Tomas (1998), Bloom Dymanics and Physiology of Gymnodinium breve with Emphasis on the Gulf of Mexico, Physiological Ecology of Harmful Algal Blooms, pp. 133-153, NATO/ASI G41

Stumpf, R., R. W. Litaker, L. Lanerolle, and P.A. Tester (2008), Hydrodynamic accumulation of Karenia off the west coast of Florida, Continental Shelf Research 28, pp. 189-213, doi:10-1016/j.csr.2007.04.017.

Stumpf, R., M. C. Tomlinson, J. A. Calkins, B. Kirkpatrick, K. Fisher, K. Nierenberg, R. Currier, and T. T. Wynne (2009), Skill assessment for an operational algal bloom forecast system, Journal of Marine Systems, Vol. 76, pp. 151-161, doi:10.1016/j.jmarsys.2008.05.016

Tester, P. A., K. Wiles, S. M. Varnam, G. V. Ortega, A. M. Dubois, and V. A. Fuentes (2004), Harmful Algal Blooms in the Western Gulf of Mexico: Karenis brevis is Messin' with Texas and Mexico!, Ecology, 2001-2002.

Weaver, S.J. and S. Nigam (2007), Variability of the Great Plains Low-Level Jet: Large Sale Circulation Context and Hydroclimate Impacts, Journal of Climate, 20, pp. 1532-1511.

Wilson, W.B. (1966), The suitability of sea-water for survival and growth of *Gymnodinium breve* Davis; and some effects of phosphorus and nitrogen on its growth, Florida Board Conserv. Mar. Lab. Prof. Pap. Ser., No. 7, 42 p.

Wynne, T. T., R. P. Stumpf, M. C. Tomlinson, V. Ransibrahmanakul, and T. A. Villareal (2005), Detecting Karenia brevis blooms and algal resuspension in the western Gulf of Mexico with satellite ocean color imagery, Harmful Algae 4, pp. 992-1003, doi:10.1016/j.hal.2005.02.004.

Wynne, T. T., R. P. Stumpf, M. C. Tomlinson, T. A. Villareal, K. Wiles, G. Heideman, M. Byrd, D. Buzan, and L. Campbell (2008), Moving Towards an Operational Harmful Algal Bloom Forecasting System in Texas (USA), in Proceedings of the 12th International Conference on Harmful Algae.International Society for the Study of Harmful Algae and Intergovernmental Oceanographic Commission of UNESCO, pp. 397, Copenhagen, Denmark.

Zhang, X., M. Marta-Almeida, and R. Hetland (2012), A high-resolution pre-operational forecast model of circulation on the Texas-Louisiana shelf and slope, Journal of Operational Oceanography, Vol. 5(1), pp. 19-34.